MRI for Detection of Hepatocellular Carcinoma: Comparison of Mangafodipir Trisodium and Gadopentetate Dimeglumine Contrast Agents

Ji Hyun Youk[1]
Jeong Min Lee[2]
Chong Soo Kim[1]

OBJECTIVE. The purpose of our study was to compare the performance of mangafodipir trisodium (Mn-DPDP)–enhanced and dynamic gadopentetate dimeglumine–enhanced MRI for the detection of hepatocellular carcinoma.

MATERIALS AND METHODS. Forty-six patients with 96 hepatocellular carcinomas underwent Mn-DPDP– and gadopentetate dimeglumine–enhanced MRI. The MRI examination included unenhanced T2-weighted turbo spin-echo and T1-weighted 2D fast low-angle shot (FLASH) sequences and a 3D FLASH sequence after the administration of gadopentetate dimeglumine and Mn-DPDP. Two observers reviewed three sets of images: a set of gadopentetate dimeglumine–enhanced MR images, a set of Mn-DPDP–enhanced MR images, and a combination of the gadopentetate dimeglumine and Mn-DPDP sets. Using receiver operating characteristic (ROC) analysis, imaging sets were compared for diagnostic accuracy and sensitivity.

RESULTS. The area under the ROC curve (A_z) was 0.942 for the gadopentetate dimeglumine–Mn-DPDP set, 0.932 for the gadopentetate dimeglumine set, and 0.877 for the Mn-DPDP set ($p < 0.05$). The mean sensitivity was greater for the gadopentetate dimeglumine set than for the Mn-DPDP set (87.5% vs 72.4%; $p < 0.05$). The false-negative rate of the Mn-DPDP set was statistically greater than that of the gadopentetate dimeglumine set (27.6% vs 12.5%). Most false-negative cases in the Mn-DPDP set were due to small (diameter < 2 cm), isoenhanced lesions.

CONCLUSION. Gadopentetate dimeglumine–enhanced MRI was superior to Mn-DPDP–enhanced MRI for the detection of hepatocellular carcinomas.

The use of MRI is increasing for the assessment of focal liver lesions, especially hepatocellular carcinoma [1–3]. However, evaluation of the liver in patients with chronic liver diseases is still a major diagnostic problem [2–4]. Patients with chronic hepatitis or cirrhosis of the liver have an increased risk of developing hepatocellular carcinoma, so early detection is mandatory for optimal treatment. This need for better detection of hepatocellular carcinoma has resulted in the use of contrast agents for MRI of the liver [5, 6]. Dynamic MRI after a bolus injection of gadopentetate dimeglumine chelates has been accepted as a valuable method for the detection and characterization of liver tumors [6–9]. The contrast effect depends on the differential distribution between normal parenchyma and tumor, which in turn depends on differences in local perfusion, capillary permeability, and interstitial leakage [10]. However, the gadopentetate dimeglumine chelates have a short imaging window of less than a few minutes after IV infusion. Therefore, to achieve the maximum effect of the contrast material, rapid imaging acquisition is essential. In clinical situations, this limits the use of high-resolution imaging, whereas the use of thick imaging sections might induce the problem of partial volume averaging.

With the recent development of liver-specific contrast agents such as superparamagnetic iron oxides and mangafodipir trisodium (Mn-DPDP), the uptake of contrast agents by functional cells has also increased the sensitivity of lesion detection and the specificity for tissue characterization [11–16]. Mn-DPDP is a paramagnetic hepatobiliary contrast agent taken up by the functioning hepatocytes and eliminated mainly by the biliary tract; it has shown its efficacy for improving the detection and delineation of liver lesions in comparison with unenhanced imaging [17–19]. To our knowledge, only one study [20] has compared gadopentetate dimeglumine–enhanced MRI

Received January 5, 2004; accepted after revision March 19, 2004.

[1]Department of Diagnostic Radiology, Chonbuk National University Hospital, Conju, South Korea.

[2]Department of Radiology and Institute of Radiation Medicine, Seoul National University Hospital, 28, Yongon-dong, Chongno-gu, Seoul 110-744, South Korea. Address correspondence to J. M. Lee (leejm@radcom.snu.ac.kr).

AJR 2004;183:1049–1054

0361–803X/04/1834–1049

and Mn-DPDP–enhanced MRI for the detection of focal liver malignancies. The comparison of these two agents for the detection of focal liver malignancies, using currently available MRI units, seems to be of clinical and financial importance.

The purpose of this study was to compare the performance of Mn-DPDP–enhanced and gadopentetate dimeglumine–enhanced MRI for the detection of hepatocellular carcinoma.

Materials and Methods

Patients

Between October 2000 and July 2002, 129 patients who were thought to have focal hepatic masses on the basis of clinical evaluation or a prior cross-sectional imaging study, underwent Mn-DPDP–enhanced and multiphase dynamic gadopentetate dimeglumine–enhanced MRI. We excluded 83 of these patients because they had a lesion confirmed as benign (n = 37: cysts [n = 15] and hemangiomas [n = 18]), a malignant mass other than hepatocellular carcinoma (n = 40: metastases [n = 35] and cholangiocarcinoma [n = 5]), or no firm evidence of a conclusive diagnosis (n = 10). Therefore, 46 patients (39 men and seven women; age range, 41–89 years; mean age, 62.1 ± 7.2 years) with a conclusive diagnosis of hepatocellular carcinoma (n = 96) were enrolled in this study. The intervals between gadopentetate dimeglumine–enhanced MRI and Mn-DPDP–enhanced MRI were less than 1 week (mean, 1.3 ± 0.2 days). The mean diameter of the tumors was 2.2 ± 1.8 cm. The number of lesions ranged from one to four in each patient. Written informed consent was obtained from all patients after the nature and purpose of the procedures had been fully explained, and the appropriate institutional review board approved this study.

Lesion Confirmation

Confirmation of the diagnosis and determination of the number and size of the hepatic lesions as a standard of reference in receiver operating characteristic (ROC) analysis were based on-site by means of interpretation of all available data in each patient by two experienced radiologists in consensus; these radiologists, who served as study coordinators, did not take part in the ROC analysis. These data included histologic analysis, all imaging data (sonography, dynamic helical CT, MRI, iodized oil–enhanced CT obtained 2 weeks after transcatheter arterial chemoembolization, digital subtraction angiography with CT arteriography, and CT portography), clinical data, laboratory data, and follow-up findings for a minimum of 6 months and a maximum of 1.5 years.

The diagnosis of hepatocellular carcinoma was based on histologic examination in 17 patients; in the remaining 29 patients, the diagnosis was based on clinical laboratory data (positive findings of hepatitis B surface antigen or hepatitis C antibody and serum α_1-fetoprotein level of > 200 ng/mL) and CT findings during hepatic arteriography and arterial portography, findings at MRI, or both or in combination with typical angiographic findings during transcatheter arterial chemoembolization (n = 9), or specific findings on iodized-oil–enhanced CT (n = 20).

MRI Examinations

All MRI examinations were performed on one of two 1.5-T MRI systems (Magnetom Vision or Magnetom Symphony, Siemens) using a phased-array multicoil. Unenhanced images included T2-weighted respiratory-triggered turbo spin-echo sequences (TR range/TE, 2,800–3,200/101; acquisition time, 16 sec; flip angle, 150°; matrix, 136 × 256) and T1-weighted fast low-angle shot (FLASH) sequences (TR/TE, 128/4.1 or 6.0; acquisition time, 17 sec; flip angle, 70° or 80°; matrix, 136 × 256) with 7-mm section thickness and a 10% gap. Multiphasic dynamic T1-weighted 3D FLASH sequences with fat saturation (3.4/1.6; acquisition time, 20 sec; flip angle, 20°; matrix, 121 × 256) were acquired before and 20, 40, and 120 sec after the rapid bolus injection of gadopentetate dimeglumine (Magnevist, Schering) at a dose of 0.1 mmol/kg using an automated injector (Medrad). The injection was followed by a 20-mL saline flush.

Mn-DPDP–enhanced MRI was performed after the infusion of 0.5 mL/kg of Mn-DPDP (Teslascan, Amersham Health) during 10 min. Fifteen to thirty minutes after the administration of the contrast agent, T1-weighted MR images were obtained using 3D FLASH and fat saturation (3.8/1.8; acquisition time, 20 sec; flip angle, 15°; matrix, 115 × 256) and 2D FLASH with and without fat saturation (166/3.8; acquisition time, 19 sec; flip angle, 70° or 80°; matrix, 115 × 256) with 7-mm section thickness and a 10% gap. The field of view was 240–270 × 300–360 mm. All patients underwent Mn-DPDP–enhanced MRI after gadopentetate dimeglumine–enhanced MRI.

MR Image Analysis

The retrospective reviewing procedure in the ROC analysis was performed independently in three sessions by two observers with experience in abdominal MRI without any clinical information or diagnosis. To limit the learning bias, the interval between sessions was at least 2 weeks, and images of one group were randomly assigned to each observer and to each session. In the first session, the two observers reviewed a set of images (gadopentetate dimeglumine set) that included both unenhanced and gadopentetate dimeglumine–enhanced images. In the second session, each observer reviewed a set of images (Mn-DPDP set) that included both unenhanced and Mn-DPDP–enhanced images of each lesion. In the third session, the observers reviewed images of the Mn-DPDP sets and the gadopentetate dimeglumine sets together. The images of all unenhanced and contrast-enhanced sequences (gadopentetate dimeglumine–Mn-DPDP set) were presented to each observer simultaneously, and the combined assessment of all images was used for scoring. Each observer recorded the number of suspected lesions seen, their size, and the segmental location of the lesions according to the classification scheme of Couinaud, and assigned each lesion a confidence rating score for the presence of hepatocellular carcinoma based on a 4-point scale as follows: 5, definitely present; 4, probably present; 3, undetermined; 2, probably not present; and 1, definitely not present.

In addition, two radiologists who did not take part in the ROC analysis evaluated all lesions that were not identified or pseudolesions that were identified by any observer on the images of the gadopentetate dimeglumine set or the Mn-DPDP set for potential explanations about why the lesions were missed or the pseudolesions were detected.

Statistical Analysis

For all image sets, alternative-free-response ROC curves were plotted for all lesions. ROC evaluation software (ROCKIT 0.9B, Charles E. Metz) was used, and the diagnostic accuracy of each image set was determined by calculating the area under the ROC curve (A_z). Differences among ROC curves were tested for significance ($p < 0.05$) using the two-tailed area test for paired data. The lesions assigned a score of 4 or 5 by each reviewer were regarded as correctly diagnosed lesions, and sensitivity values were calculated on this basis. Also, false-positive and false-negative values were obtained for each image set. Differences in calculated values in the detection of hepatocellular carcinoma were tested for significance ($p < 0.05$) by performing the two-tailed Student's t test.

The kappa statistic was used to measure the degree of agreement among the observers, and kappa values greater than 0 were considered to indicate positive correlation. Measurements were rated as follows: kappa values of 0.31–0.60, good correlation; 0.61–0.90, very good correlation; and greater than 0.90, excellent correlation.

Results

ROC Analysis

The calculated A_z values for hepatocellular carcinoma are shown in Table 1. The corresponding ROC curves formed on the basis of pooled data from the two observers for the gadopentetate dimeglumine–Mn-DPDP set, the gadopentetate dimeglumine set, and the Mn-DPDP set are shown in Figure 1. The gadopentetate dimeglumine–Mn-DPDP set performed best in the ROC analysis, followed by the gadopentetate dimeglumine set and then by the Mn-DPDP set (Fig. 1). The gadopentetate dimeglumine set (mean A_z = 0.932) was statistically superior to the Mn-

TABLE 1 Comparison of Mangafodipir Trisodium (Mn-DPDP)–Enhanced and Gadopentetate Dimeglumine–Enhanced MRI for Diagnostic Accuracy

Image Set Enhanced with	Area Under Receiver Operating Characteristic Curve			
	Observer 1	Observer 2	Mean	κ
Gadopentetate dimeglumine	0.961 ± 0.01[a]	0.906 ± 0.02[a]	0.932 ± 0.01[a]	0.521 ± 0.05
Mn-DPDP	0.879 ± 0.02	0.875 ± 0.02	0.877 ± 0.02	0.630 ± 0.05
Gadopentetate dimeglumine and Mn-DPDP	0.980 ± 0.01[a]	0.905 ± 0.02[a]	0.942 ± 0.01[a]	0.574 ± 0.04

Note.—Data are mean ± SD.

[a]Significant ($p < 0.05$) difference between these images and those enhanced with Mn-DPDP.

DPDP set (mean A_z = 0.877) ($p < 0.01$). However, no significant differences were seen between the gadopentetate dimeglumine–Mn-DPDP set (mean A_z = 0.942) and the gadopentetate dimeglumine set in the diagnostic accuracy of hepatocellular carcinoma. The interobserver variability showed good agreement between the two observers (Table 1).

Sensitivity and False-Positive and False-Negative Values

Table 2 summarizes the sensitivity and false-positive and false-negative values of the contrast-enhanced image sets in the detection of hepatocellular carcinoma determined using the results of ROC analysis on the basis of scores of 4 or 5 assigned by the two observers. The best sensitivity was achieved for the gadopentetate dimeglumine–Mn-DPDP set (88.0%). The sensitivity of both the gadopentetate dimeglumine–Mn-DPDP set and the gadopentetate dimeglumine set (87.5%) was significantly superior to that of the Mn-DPDP set (72.4%) ($p < 0.05$).

The false-positive rate of the gadopentetate dimeglumine set was statistically greater than that of the Mn-DPDP set. The main cause of false-positive cases in the gadopentetate dimeglumine set was an arterioportal shunt (69%, 31/45) (Fig. 2). The false-negative rate of the Mn-DPDP set was statistically greater than that of the gadopentetate dimeglumine set. Most false-negative cases in the Mn-DPDP set were the result of a small (diameter < 2 cm), isoenhanced lesion (83%, 19/23) (Fig. 3).

Discussion

The liver is a common site of both primary and metastatic tumors. Reliable liver imaging, both morphologic and functional, is important for effective use of treatments such as chemotherapy, percutaneously delivered ablative procedures, or surgical resection, and for the evaluation of their effects [21, 22]. The optimal technique should allow a precise description of the number of focal lesions and their anatomic details and preferably should provide information on the differential diagnosis and organ function [23, 24]. Although unenhanced MRI using recently developed imaging techniques can equal or exceed the accuracy of contrast-enhanced CT for the detection and characterization of liver tumors, liver tumor detection can be further improved by pharmaceutic manipulation of tissue proton relaxation using paramagnetic or superparamagnetic MRI contrast agents [25].

Mn-DPDP is a hepatocyte-specific contrast agent capable of increasing the signal intensity of normal liver. At present, the best clinical role for this agent appears to be in improving detection of the number and extent of focal liver lesions in patients in whom hepatic resection is being contemplated [15, 26]. Also, Mn-DPDP–enhanced MRI can characterize lesions to a greater degree than unenhanced imaging can—that is, tumors of hepatocytic origin, such as hepatocellular carcinoma, hepatic adenoma, or focal nodular hyperplasia, that retain sufficient hepatocyte function actually take up the contrast agent and appear brighter on T1-weighted images than those of nonhepatocytic origin, such as metastases, cholangiocarcinomas, and cysts [15, 18]. But gadopentetate dimeglumine–enhanced MRI is used for routine MRI examination of the liver, and the most compelling case for the routine use of gadopentetate dimeglumine chelates is examination of the liver in patients who are thought to have hepatocellular carcinoma [27].

In our study, using ROC analysis we attempted to compare the diagnostic accuracy of Mn-DPDP–enhanced MRI with that of dynamic gadopentetate dimeglumine–enhanced MRI for the detection of hepatocellular carcinoma. For the diagnosis of hepatocellular carcinoma, the gadopentetate dimeglumine set was significantly more accurate and more sensitive than the Mn-DPDP set ($p < 0.05$). These results agreed with the results of the previous report by Kettritz et al. [20].

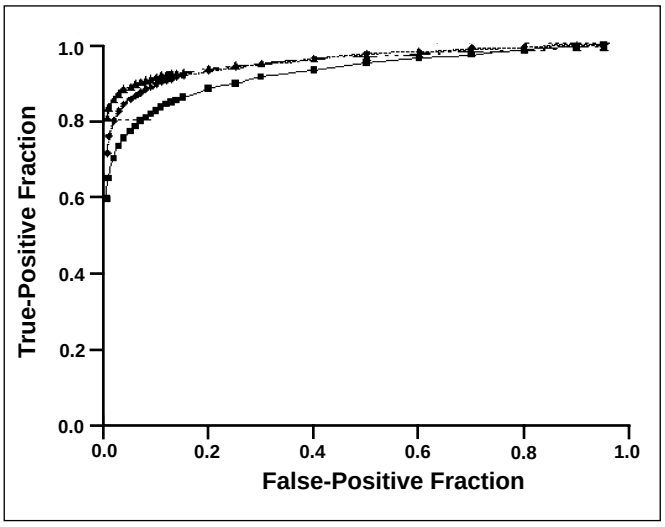

Fig. 1.—Results of receiver operator characteristic (ROC) analysis. Graph of mean area under ROC curves (A_z) with pooled data of two observers indicates diagnostic accuracy of gadopentetate dimeglumine–mangafodipir trisodium (Mn-DPDP) set (▲), gadopentetate dimeglumine set (◆), and Mn-DPDP set (■).

TABLE 2 **Comparison of Mangafodipir Trisodium (Mn-DPDP)–Enhanced and Gadopentetate Dimeglumine–Enhanced MRI for Sensitivity and False-Positive and False-Negative Values**

Image Set Enhanced with	Sensitivity (%)	False-Positive Value (%)	False-Negative Value (%)
Gadopentetate dimeglumine	87.5[a]	7.1[a]	12.5[a]
Mn-DPDP	72.4	2.1	27.6
Gadopentetate dimeglumine and Mn-DPDP	88.0[a]	2.2	12.0

[a]Significant ($p < 0.05$) difference between these images and those enhanced with Mn-DPDP.

Several factors make gadopentetate dimeglumine–enhanced MRI superior to Mn-DPDP–enhanced MRI for diagnostic accuracy in hepatocellular carcinomas. First, depending on the amount of uptake of the contrast agent, hepatocellular carcinoma may become hyperintense, hypointense, or isointense on Mn-DPDP–enhanced MR images [16]. If the image shows greater or less enhancement than liver parenchyma, or an obvious hypointense capsule on Mn-DPDP–enhanced MRI, hepatocellular carcinoma can be reliably identified [18]. However, because of their enhancement that is as much as that of background liver parenchyma and that becomes isointense, some hepatocellular carcinomas, particularly small lesions, may be obscured on Mn-DPDP–enhanced MRI, which would make the false-negative rate for Mn-DPDP–enhanced MRI greater than that for gadopentetate dimeglumine–enhanced MRI [16] (Fig. 3). Second, although the ultimate usefulness of Mn-DPDP for detecting hepatocellular carcinoma in patients with cirrhosis remains to be determined, some authors have reported that benign hepatocellular lesions, including regenerating nodules without iron deposits, may have homogeneous, hyperintense enhancement simulating that of some hepatocellular carcinomas, and it can be difficult to differentiate these benign lesions from hepatocellular carcinoma after the administration of Mn-DPDP [10, 13–15, 17, 28, 29].

However, Mn-DPDP–enhanced MRI was helpful in decreasing the false-positive diagnoses (Table 2). Most of the false-positives on gadopentetate dimeglumine–enhanced MRI seemed to result from perfusion abnormalities such as an arterioportal shunt of the liver parenchyma. On Mn-DPDP–enhanced MRI, the arterioportal shunt was not depicted and the liver parenchyma showed relatively homogeneous enhancement (Fig. 2). Also, Mn-DPDP successfully shows im-

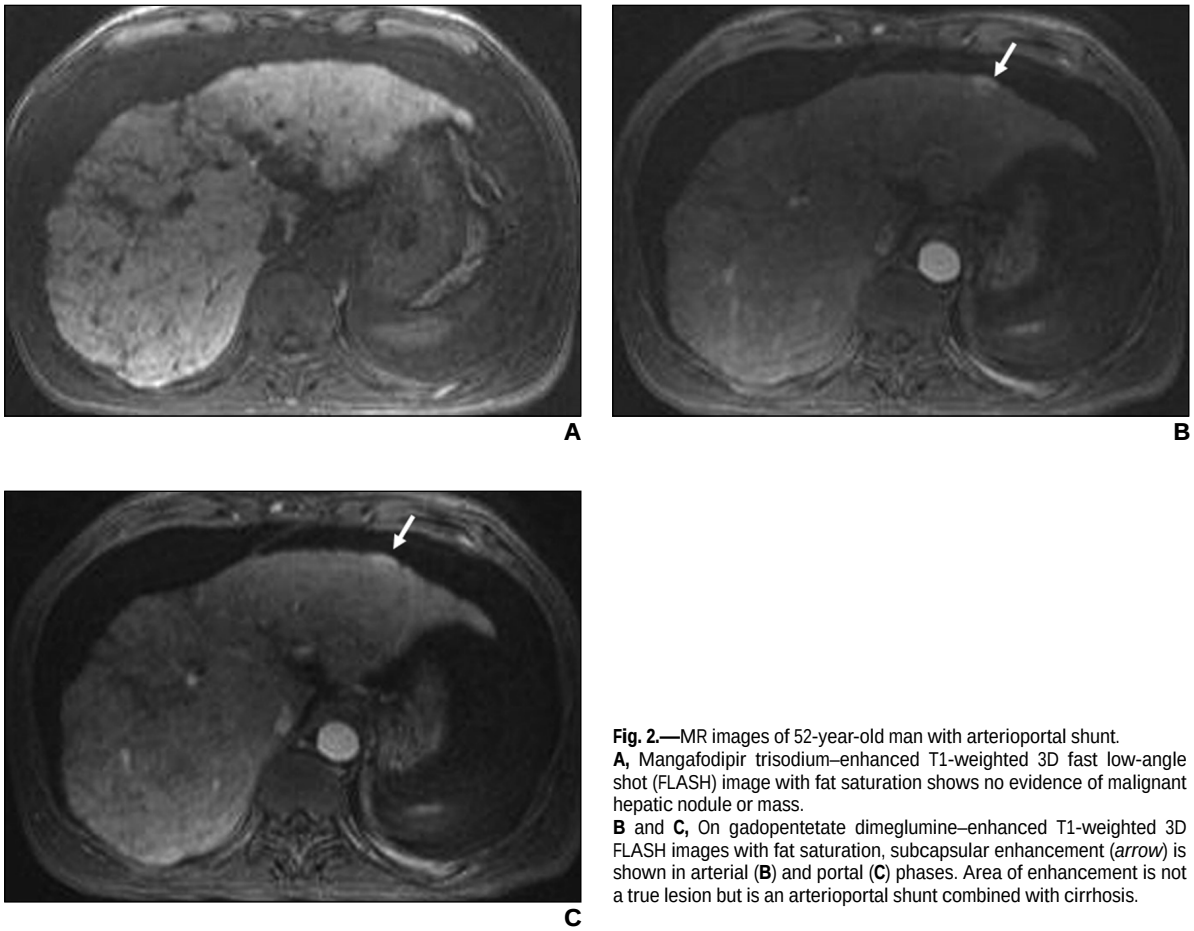

Fig. 2.—MR images of 52-year-old man with arterioportal shunt.
A, Mangafodipir trisodium–enhanced T1-weighted 3D fast low-angle shot (FLASH) image with fat saturation shows no evidence of malignant hepatic nodule or mass.
B and **C,** On gadopentetate dimeglumine–enhanced T1-weighted 3D FLASH images with fat saturation, subcapsular enhancement (*arrow*) is shown in arterial (**B**) and portal (**C**) phases. Area of enhancement is not a true lesion but is an arterioportal shunt combined with cirrhosis.

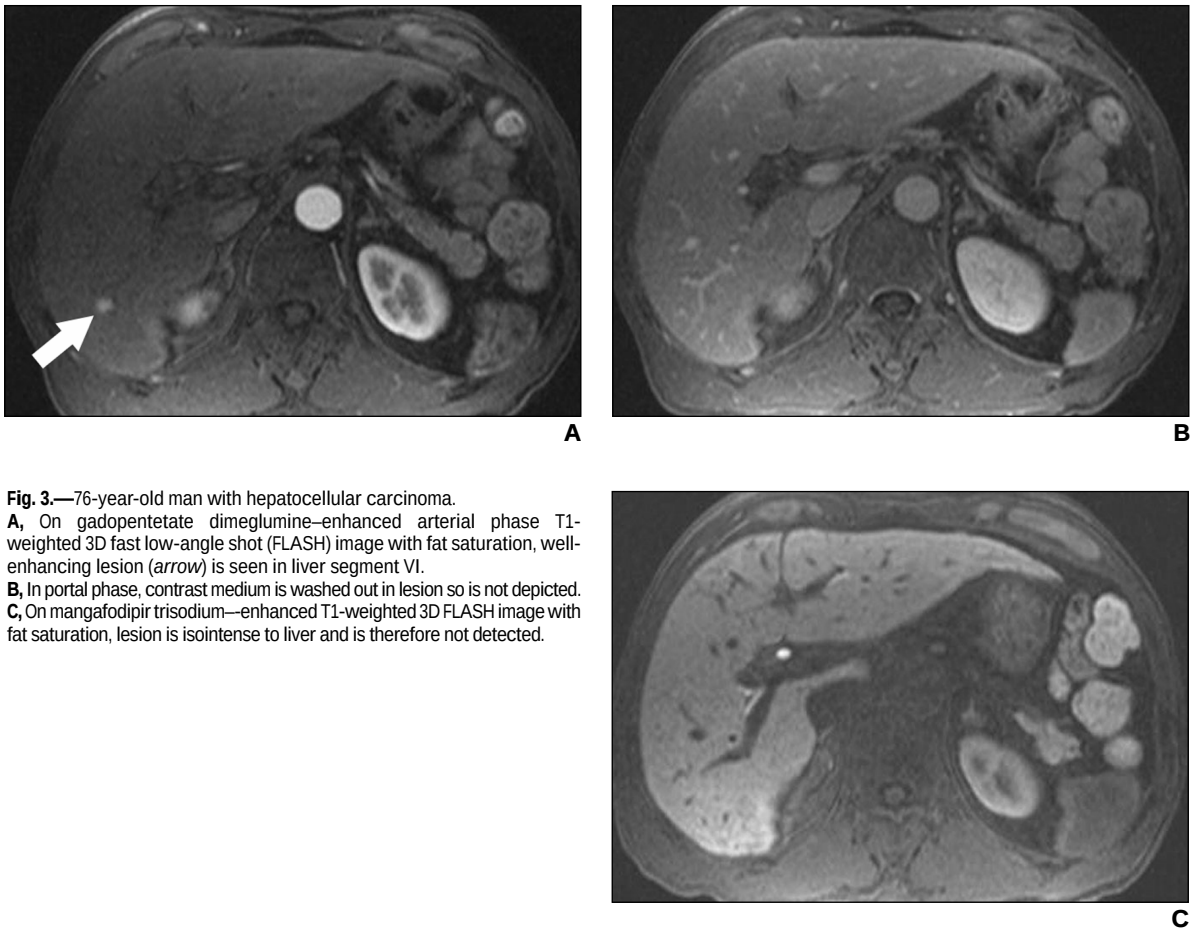

Fig. 3.—76-year-old man with hepatocellular carcinoma.
A, On gadopentetate dimeglumine–enhanced arterial phase T1-weighted 3D fast low-angle shot (FLASH) image with fat saturation, well-enhancing lesion (*arrow*) is seen in liver segment VI.
B, In portal phase, contrast medium is washed out in lesion so is not depicted.
C, On mangafodipir trisodium—enhanced T1-weighted 3D FLASH image with fat saturation, lesion is isointense to liver and is therefore not detected.

proved conspicuity and delineation of many liver lesions [16–18].

We also assessed the performance of a combined gadopentetate dimeglumine–Mn-DPDP set for its diagnostic accuracy using ROC analysis. The diagnostic accuracy of the gadopentetate dimeglumine–Mn-DPDP set was the best, and the false-positive value of the gadopentetate dimeglumine–Mn-DPDP set was as low as that of the Mn-DPDP set. From the results, Mn-DPDP–enhanced MRI is expected to have an axillary role for the diagnosis of hepatocellular carcinoma.

Our study has a number of limitations. First, the lesions of 29 patients were not pathologically proven. To have the best achievable gold standard, typical clinical and laboratory findings, in combination with typical findings of other imaging techniques, are used as the diagnostic criteria, but careful follow-up was performed in these patients. However, the possibility cannot be totally excluded that not all the lesions actually existed or, if they existed, were hepatocellular carcinomas. Also, we do not know about tumoral differentiation in hepatocellular carcinomas, which would be helpful for analyzing our results because the degree of enhancement on Mn-DPDP–enhanced MRI might be related to the differentiation of hepatocellular carcinomas. Second, many patients had hepatic dysfunction that might limit the degree of enhancement of the liver parenchyma and lower the diagnostic efficacy of Mn-DPDP. Last, because the study was performed retrospectively and excluded benign lesions such as hemangiomas or cysts from the analysis, a selection bias may exist and may limit the extrapolation of the data of this study to clinical situations.

In conclusion, multiphase dynamic gadopentetate dimeglumine–enhanced MRI was superior to Mn-DPDP–enhanced MRI; Mn-DPDP–enhanced MRI had only a limited role in the diagnosis of hepatocellular carcinoma.

Acknowledgment

We thank Bonnie Hami, Department of Radiology, University Hospitals of Cleveland, Cleveland, OH, for her editorial assistance and manuscript preparation.

References

1. Mergo PJ, Ros PR. Imaging of diffuse liver disease. *Radiol Clin North Am* 1998;36:365–375
2. Sharma R, Saini S. Role and limitations of magnetic resonance imaging in the diagnostic work-up of patients with liver cancer. *J Comput Assist Tomogr* 1999;23[suppl]:S39–S44
3. Solbiati L, Cova L, Ierace T, Marelli P, Dellanoce M. Liver cancer imaging: the need for accurate detection of intrahepatic disease spread. *J Comput Assist Tomogr* 1999;23:S29–S37
4. Frazer C. Imaging of hepatocellular carcinoma. *J Gastroenterol Hepatol* 1999;14:750–756
5. Semelka RC, Worawattanakul S, Kelekis NL, et al. Liver lesion detection, characterization, and effect on patient management: comparison of single-phase spiral CT and current MR techniques. *J Magn Reson Imaging* 1997;7:1040–1047
6. Semelka RC, Shoenut JP, Kroeker MA, et al. Focal liver disease: comparison of dynamic contrast-enhanced CT and T2-weighted fat-suppressed, FLASH, and dynamic gadolinium-enhanced MR imaging at 1.5T. *Radiology* 1992;184:687–694

7. Yamashita Y, Fan ZM, Yamamoto H, et al. Spin-echo and dynamic gadolinium-enhanced FLASH MR imaging of hepatocellular carcinoma: correlation with histopathologic findings. *J Magn Reson Imaging* 1994;4:83–90
8. Yamashita Y, Hatanaka Y, Yamamoto H, et al. Differential diagnosis of focal liver lesions: role of spin-echo and contrast-enhanced dynamic MR imaging. *Radiology* 1994;193:59–65
9. Hamm B, Thoeni RF, Gould RG, et al. Focal liver lesions: characterization with nonenhanced and dynamic contrast material-enhanced MR imaging. *Radiology* 1994;190:417–423
10. Clement O, Siauve N, Cuenod CA, Vuillemin-Bodaghi V, Leconte I, Frija G. Mechanisms of action of liver contrast agents: impact for clinical use. *J Comput Assist Tomogr* 1999;23[suppl]:S45–S52
11. Hamm B, Vogl TJ, Branding G, et al. Focal liver lesions: MR imaging with Mn-DPDP—initial clinical results in 40 patients. *Radiology* 1992;182:167–174
12. Rummeny E, Ehrenheim C, Gehl HB, et al. Manganese-DPDP as a hepatobiliary contrast agent in the magnetic resonance imaging of liver tumors: results of clinical phase II trials in Germany including 141 patients. *Invest Radiol* 1991;26[suppl]:S142–S145
13. Bernardino ME, Young SW, Lee JK, Weinreb JC. Hepatic MR imaging with Mn-DPDP: safety, image quality, and sensitivity. *Radiology* 1992;183:53–58
14. Vogl TJ, Hamm B, Schnell B, et al. Mn-DPDP enhancement patterns of hepatocellular lesions on MR images. *J Magn Reson Imaging* 1993;3:51–58
15. Rofsky NM, Weinreb JC, Bernardino ME, Young SW, Lee JK, Noz ME. Hepatocellular tumors: characterization with Mn-DPDP-enhanced MR imaging. *Radiology* 1993;188:53–59
16. Liou J, Lee JK, Borrello JA, Brown JJ. Differentiation of hepatomas from nonhepatomatous masses: use of MnDPDP-enhanced MR images. *Magn Reson Imaging* 1994;12:71–79
17. Grant D, Refsum H, Rummeny E, Marchal G. The need for effective contrast agents to enhance the performance of MR imaging. *Acta Radiol* 1997;38:623–625
18. Rummeny EJ, Torres CG, Kurdziel JC, Nilsen G, Op de Beeck B, Lundby B. MnDPDP for MR imaging of the liver: results of an independent image evaluation of the European phase III studies. *Acta Radiol* 1997;38:638–642
19. Murakami T, Baron RL, Peterson MS, et al. Hepatocellular carcinoma: MR imaging with mangafodipir trisodium (Mn-DPDP). *Radiology* 1996;200:69–77
20. Kettritz U, Schlund JF, Wilbur K, Eisenberg LB, Semelka RC. Comparison of gadolinium chelates with manganese-DPDP for liver lesion detection and characterization: preliminary results. *Magn Reson Imaging* 1996;14:1185–1190
21. Baker ME, Pelley R. Hepatic metastases: basic principles and implications for radiologists. *Radiology* 1995;197:329–337
22. Bennett WF, Bova JG. Review of hepatic imaging and a problem-oriented approach to liver masses. *Hepatology* 1990;12:761–775
23. Utsunomiya T, Matsumata T, Adachi E, Honda H, Sugimachi K. Limitations of current preoperative liver imaging techniques for intrahepatic metastatic nodules of hepatocellular carcinoma. *Hepatology* 1992;16:694–701
24. Rummeny EJ, Wernecke K, Saini S, et al. Comparison between high-field-strength MR imaging and CT for screening of hepatic metastases: a receiver operating characteristics analysis. *Radiology* 1992;182:879–886
25. Brasch R. New directions in the development of MR imaging contrast media. *Radiology* 1992;183:1–11
26. Wang C, Ahlstrom H, Ekholm S, et al. Diagnostic efficiency of Mn-DPDP in MR imaging of the liver: a phase III multicentre study. *Acta Radiol* 1997;38:643–649
27. Oi H, Murakami T, Kim T, Matsushita M, Kishimoto H, Nakamura H. Dynamic MR imaging and early-phase helical CT for detecting small intrahepatic metastases of hepatocellular carcinoma. *AJR* 1996;166:369–374
28. Larson RE, Semelka RC, Bagley AS, Molina PL, Brown ED, Lee JK. Hypervascular malignant liver lesions: comparison of various MR imaging pulse sequences and dynamic CT. *Radiology* 1994;192:393–399
29. King LJ, Burkill GJC, Scurr ED, Vlavianos P, Murray-Lyons I, Healy JC. MnDPDP enhanced magnetic resonance imaging of focal liver lesions. *Clin Radiol* 2002;57:1047–1057